

ENERGY DECAY MECHANISMS AND ANHARMONIC LATTICE DYNAMICS: THE CASE OF SOLID NITROGEN

G.F. SIGNORINI, P.F. FRACASSI, R. RIGHINI

Dipartimento di Chimica, Università di Firenze, via G. Capponi 9, 50121 Florence, Italy

and

R.G. DELLA VALLE

Istituto di Chimica Fisica, Università di Bologna, viale Risorgimento 4, 40136 Bologna, Italy

Received 12 June 1985

The anharmonic frequencies and linewidths of the lattice phonons in α -N₂ are calculated on the basis of three different intermolecular potentials which include atom–atom and electrostatic interactions. The distinction between stationary anharmonicity and decay anharmonicity is stressed, and the mechanism of energy transfer between the optical lattice phonons and the two-phonon manifold of the crystal is discussed in detail. The temperature dependence of the phonon self-energy is also considered. The results thus obtained for α -N₂ are compared with predictions from previous lattice dynamics, SCP and molecular dynamics calculations. The calculated anharmonic effects are substantially independent of the adopted potential: the agreement with experimental data is reasonably good as far as the linewidths are concerned, while the anharmonic deformation of the potential wells (and thus the frequency shifts) is overestimated. We suggest that, while higher orders in the diagram expansion are necessary for a proper account of the stationary anharmonicity, the decay anharmonicity limits its effectiveness to two-phonon processes, thus allowing proper predictions of the phonon lifetimes by using the lowest-order diagrams. Finally, α -N₂ is compared to α -CO, and the role played by the translation–rotation coupling is discussed.

1. Introduction

The dynamical properties of condensed molecular systems are currently analyzed in terms of pairwise additive effective potentials [1]. Ideally, one should derive a model for the intermolecular interactions able to account for the collective dynamics, the evolution and decay of the excitations, and the structural transformations consequent to changes in the thermodynamical coordinates.

The approximations involved in each method critically affect the nature of the conclusions. A model may be satisfactory in describing a specific situation (or several features of a specific situation), while neglecting factors which become dominant under different conditions. It is therefore of great value to explore limits and implications of different approaches, in order to extract the in-

formation hidden in the hypotheses.

The molecular motions are determined by the (instantaneous) potential well seen by each molecule as an effect of its interactions with all the others. In most cases, especially at low temperatures, the molecules are localized in rather deep potential wells, and the occurrence of spatial symmetry allows the distinction between different “modes” of the system. As long as it is meaningful to individually characterize these modes, it is also meaningful to think in terms of “coupling of the modes” and of “mode decay”. The dynamics of the system can be described within an “harmonic” approximation (i.e. as the superposition of individual excitations), and the decay of each excitation can be treated by means of perturbative methods.

At higher temperatures, and generally in the proximity of phase transitions, “anharmonicity”

becomes a dominant factor. By "anharmonicity" we mean two distinct (although usually coexisting) cases:

(i) Due to the amplitude of the molecular displacements, the potential well seen by each molecule is deformed from a parabolic shape. The corresponding energy levels are shifted with respect to the harmonic values.

(ii) The coupling between the modes induces finite lifetimes of the excitations above (or below) the thermal bath, and thus a redistribution of the total energy of the system. The time-dependence of the motion deviates from an $\exp(i\omega t)$ law. Its Fourier transform is no more a Dirac's delta function, but rather becomes a distribution usually characterized by a peak with finite width, centred at a shifted "main" frequency.

(i) and (ii) generally coexist, and generate analogous observable effects (line broadening and frequency shift) but are not necessarily consequent on each other: (i) accounts for the stationary properties of the system, and redefines the nature of each single mode, while (ii) describes the coupling between different modes and, thus, the occurrence of the energy decay. In this sense, it is meaningful to distinguish between the "stationary" anharmonicity (i) and the time-dependent one (ii). In case of very large couplings, the modes are no more characterized individually, the very symmetry imposed to the system is violated, and the adopted picture loses its meaning.

The intermolecular potentials are usually derived by fitting some experimental data, making use of heuristic hypotheses (such as the localization on the molecule of the interaction centres, and the analytic form of the functions describing these partial interactions), and adapting their properties to the symmetry of the molecule in the solid. It is not surprising that, quite often, a model which is successful on reproducing certain properties, does not yield proper predictions once the physical conditions are changed.

Of great importance in order to test the meaning of a model is its capability of reproducing the dependence of an observable from the thermodynamical coordinates. Thus, methods which allow such analysis are of extreme value.

The present paper is mainly concerned with the

use of anharmonic lattice dynamics methods; the results of such calculations are discussed and compared to the information obtained from other approaches.

We shall consider the case of solid nitrogen in its α phase. Much work has been devoted to this system which, in many aspects, still poses substantial problems. Solid nitrogen undergoes many structural transformations by changing both the external pressure and the temperature. Even at low temperatures the molecules exhibit rather large librational motions, suggesting that anharmonic effects are important also at temperatures close to the absolute zero.

Many different intermolecular potentials have been proposed and utilized with various methods (lattice dynamics, self-consistent and mean-field approaches, molecular dynamics). While several features of the system can be accounted for, none of these approaches has yet provided a globally satisfactory description of solid nitrogen.

2. Anharmonic lattice dynamics

The lattice dynamics approach to molecular solids is based upon the expansion of the crystal hamiltonian into a power series of the molecular coordinates [1]:

$$H = T + V_2 + \epsilon V_3 + \epsilon^2 V_4 + \dots, \quad (1)$$

where T is the kinetic energy, V the potential energy, and ϵ the power expansion parameter.

The elementary excitations of the lattice are the harmonic phonons (obtained by diagonalizing the crystal hamiltonian up to the second order in the coordinate expansion). Phonons interact via the high-order (anharmonic) terms of the potential.

Optical and neutron spectroscopies, being dominated by single-phonon scattering, are conveniently described in terms of single-phonon propagators. According to the many-body theory [2], the single-particle excitation is described by the statistical phonon propagator $G_i(\omega)$ (where i labels both the mode and the wave vector). G_i obeys a Dyson equation of the kind [3,4]:

$$G_i(\omega) = G_i^0(\omega) + G_i^0(\omega) \Sigma_i(\omega) G_i(\omega), \quad (2)$$

where G_i^0 is the free phonon (harmonic) propagator, and $\Sigma_i = \Delta_i + i\Gamma_i$ is the proper phonon self-energy, obtained from the sum of all proper diagrams (connected diagrams without self-energy insertions). In practice, the summation should be truncated once the convergence of Σ_i is achieved.

According to the linear response theory [5], the single-phonon bandshape is proportional to:

$$W_i(\omega) = 2\omega_i \operatorname{Im}[\omega^2 - \omega_i^2 - 2\omega_i \Sigma_i(\omega)]^{-1}. \quad (3)$$

A correct solution of the Dyson equation (2) implies a self-consistent approach, where each diagram is evaluated making use of the full-phonon propagator G_i . In practice, the diagrams (and, thus, the various densities of states) are accounted for on the basis of the free (harmonic) solutions. This is accurate as long as the corrections to G_i^0 are small, i.e. if the convergence of the perturbative expansion is achieved after the evaluation of the lowest-order diagrams.

The many-body formalism allows the rigorous distinction between what we have called stationary anharmonicity (i) and decay anharmonicity (ii). Actually, two kinds of diagrams can be distinguished [6]: those which are invariant under time reversal, and those which are not (in this respect, one must bear in mind that all phonon lines are oriented according to their wavevectors). The first set of diagrams contributes only to the real part Δ_i of the self-energy, and describes the effects of the elastic processes (stationary anharmonicity (i)); the other set introduces an imaginary contribution $i\Gamma_i$ as well, and describes the effect of decay processes. Δ_i has the effect of shifting the band peak frequency, while Γ_i results in the broadening of the line, as a consequence of the finite lifetime of the excitation.

In table 1 are summarized the lowest-order diagrams, together with their schematic contributions to Σ_i . Those representing decay processes involve averages over n -phonon densities of states. Their imaginary part (proportional to the damping Γ_i) is subject to energy conservation requirements (Dirac's delta distributions of sums and differences of phonon states), while the resonance are not involved in the calculation of the real part (proportional to the shift Δ_i). Stationary processes

imply only averages over the one-phonon density of states.

Analytic expressions for the (thermally averaged) phonon self-energy are derived in many standard texts [1,4,6]. Limiting ourselves to the lowest-order diagrams (a), (b) and (c) in table 1, we have:

$$\begin{aligned} \Sigma_{i0}^{(3)}(\omega) &= \lim_{\epsilon \rightarrow 0} \left\{ -18\hbar^{-2} \sum_{\mathbf{k}} \sum_{jh} \left| B^{(3)} \begin{pmatrix} i & j & h \\ \mathbf{0} & \mathbf{k} & -\mathbf{k} \end{pmatrix} \right|^2 \right. \\ &\quad \times \left\{ (\bar{n}_j + \bar{n}_h + 1) [(\omega + \omega_j + \omega_h + i\epsilon)^{-1} \right. \\ &\quad \left. \left. - (\omega - \omega_j - \omega_h + i\epsilon)^{-1}] \right. \right. \\ &\quad \left. \left. + (\bar{n}_j - \bar{n}_h) [(\omega - \omega_j + \omega_h + i\epsilon)^{-1} \right. \right. \\ &\quad \left. \left. - (\omega + \omega_j - \omega_h + i\epsilon)^{-1}] \right\} \right\}, \quad (4a) \end{aligned}$$

$$\begin{aligned} \Sigma_{i0}^{(3)} &= -36\hbar^{-2} \sum_{\mathbf{k}} \sum_{jh} B^{(3)} \begin{pmatrix} i & i & j \\ \mathbf{0} & \mathbf{0} & \mathbf{0} \end{pmatrix} \\ &\quad \times B^{(3)} \begin{pmatrix} j & h & h \\ \mathbf{0} & \mathbf{k} & -\mathbf{k} \end{pmatrix} (\bar{n}_h + 1) P(\omega_j)^{-1}, \quad (4b) \end{aligned}$$

$$\begin{aligned} \Sigma_{i0}^{(4)} &= 12\hbar^{-1} \sum_{\mathbf{k}} \sum_j B^{(4)} \begin{pmatrix} i & i & j & j \\ \mathbf{0} & \mathbf{0} & \mathbf{k} & -\mathbf{k} \end{pmatrix} \\ &\quad \times (2\bar{n}_j + 1), \quad (4c) \end{aligned}$$

where i, j, h and \mathbf{k} label the phonon modes and the wave vector, respectively, $n_i = [\exp(\hbar\omega_i/k_B T) - 1]^{-1}$ is the mean phonon occupation number at the temperature T , and we have employed the complex distribution:

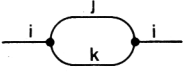
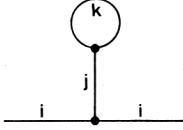
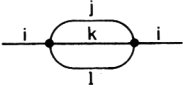
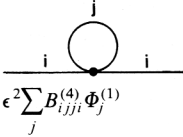
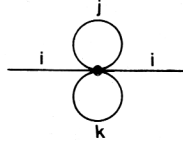
$$\lim_{\epsilon \rightarrow 0^+} (x - i\epsilon)^{-1} = P(1/x) + i\pi\delta(x), \quad (5)$$

where P denotes the Cauchy's principal part, and δ is the Dirac's delta distribution.

The term (4b), arising from diagram (b) of table 1 vanishes identically for the centrosymmetric sys-

Table 1

Contributions to the proper self-energy $\Sigma_i = \Delta_i + i\Gamma_i$ ^{a)}

Decay processes Complex contributions to Σ_i	Stationary processes Real contributions to Σ_i
 $\epsilon^2 \sum_{jk} B_{ijk}^{(3)} ^2 \Delta_{ijk} \Phi_{jk}^{(2)} \quad (a)$	 $\epsilon^2 \sum_{jk} B_{iji}^{(3)} B_{kjk}^{(3)} \Phi_j^{(1)} \Phi_k^{(1)} \quad (b)$
 $\epsilon^4 \sum_{jkl} B_{ijkl}^{(4)} ^2 \Delta_{ijk} \Phi_{jkl}^{(3)} \quad (d)$	 $\epsilon^2 \sum_j B_{ijji}^{(4)} \Phi_j^{(1)} \quad (c)$
	 $\epsilon^4 \sum_{jk} B_{ijjkkk}^{(6)} \Phi_j^{(1)} \Phi_k^{(1)} \quad (e)$

^{a)} ϵ : potential expansion parameter; $\epsilon^{m-2} B_{ij\ldots}^{(m)}$: m th order coupling coefficient; $\Phi_{ij\ldots}^{(m)}$: m -phonon density of states; $\Delta_{ij\ldots} = P[\omega_i + \omega_j + \cdots]^{-1} + i\pi\delta(\omega_i + \omega_j + \cdots)$: complex Dirac distribution. The indexes i, j, k , and l label both the mode and the wave vector. At each vertex, the total wave vector is conserved, due to lattice translational invariance.

tems, and in general yields small contributions to Δ_i when high-symmetry crystals are involved.

The next two terms in the expansion [diagrams (d) and (e) in table 1, where we have neglected diagrams analogous to (b)], yield the corrections due to three-phonon decay and four-phonon elastic scattering, respectively. The contributions arising from these diagrams are in most cases assumed negligible. This may be incorrect when large anharmonicity occurs, so that problems may arise for the convergence of the self-energy. In such cases, however, a distinction can be made between the real (Δ_i) and imaginary (Γ_i) parts of Σ_i . In fact, while $\Delta_i^{(4)}$ and $\Delta_i^{(6)}$ (from diagrams (d) and (e) respectively) are determined by the whole three-phonon and one-phonon densities of states, only the low-frequency region of the three-phonon density (a minor part of the whole density, dominated by the acoustic modes) contributes to the damping

$\Gamma_i^{(4)}$, owing to the resonance conditions (Dirac's delta distribution) contained in its expression. Energy conservation requirements, thus, drastically reduce the contributions to the linewidth due to quartic- and higher-order terms of the anharmonic expansion; as a consequence, the convergence of the damping Γ_i is substantially speeded up with respect to the shift Δ_i .

3. Solid nitrogen

The structure and phase diagram of condensed nitrogen has been extensively investigated by means of calorimetric measurements [7], electron [8] and X-ray [9] diffraction, and Raman spectroscopy [10].

Solid nitrogen exists in four crystal forms depending on pressure and temperature: at low tem-

perature and pressure it is an ordered cubic system (phase α , space group Pa3), which transforms into an ordered tetragonal crystal above ≈ 0.4 GPa (phase γ , P4₂/mmn); adjacent to the melting curve it exists as a disordered hexagonal system (phase β , P6₃/mmc) and, above 4.5 GPa at room temperature, it becomes a plastic pseudo-cubic solid (phase δ , "Pm3n").

Under its own vapour pressure, α -N₂ exists between 0 and 35.61 K [7,11]: it is a centrosymmetric cubic crystal belonging to the space group T_n⁶/Pa3, with four molecules per unit cell. The molecules are aligned along the $\langle 111 \rangle$ body diagonals, and the nitrogen atoms occupy positions of type c. The lattice constant at 0 K is 5.649 Å [11] and the bondlength in the gas phase is 1.0976 Å [12].

The factor group analysis of the $k = 0$ crystal modes yields the following representation:

$$\Gamma = A_g + A_u + E_g + E_u + 3F_g + 3F_u,$$

with five Raman-active modes (two internal stretching vibrations A_g and F_g , and three librations E_g and two F_g), two infrared-active modes (two translations F_u), two optically inactive translations A_u and E_u , and one acoustic mode F_u .

Infrared [13], Raman [14,15] and inelastic neutron scattering [16] spectra for the lattice mode region have been reported. The Kjems and Dolling neutron scattering experiment [16] provides information on the acoustic dispersions and on the phonon frequencies at the high-symmetry points of the Brillouin zone.

NQR measurements of the order parameter for α -nitrogen [17] show that the librations around the $\langle 111 \rangle$ orientations are characterized by rather large amplitudes even at low temperature (the order parameter at 0 K is judged to be $f = 0.86$ [11], corresponding to a root-mean-square angular amplitude of 12°). The order parameter decreases significantly on approaching the α - β transition.

An extensive literature is devoted to the study of the librational properties of solid nitrogen [11]. Most theoretical work has been concerned with potential models able to reproduce the frequencies of the centre of the Brillouin zone and, possibly, to account for the structural transformations of the system.

It is difficult to identify a unitary picture in the existing theoretical investigations on solid nitrogen. The very existence of so many phases clearly denotes that the dynamics of solid nitrogen is critically dominated by different factors, whose relative importance changes with the thermodynamical conditions.

Since the first calculations by Kohin [18], a separation between librations and translations has often been imposed [19,20], stressing the importance of a libron picture for α -N₂ [21–23]. Conventional quasi-harmonic lattice dynamics [16,24], which naturally includes the translation–rotation coupling, has often been criticized on the ground of the large librational amplitudes of the nitrogen molecules.

SCP [21], mean-field [23], time-dependent RPA (applied to mean-field librational and translational states [22]) calculations have been performed, and the role of anisotropic interactions is acknowledged as a fundamental issue [24–27]. The stability and dynamical evolution of the system has been investigated with molecular dynamics (MD) simulations for the α phase [28,29] and for the high-pressure phases [30], and the role played in this respect by the translation–rotation coupling has been stressed [31]. More recently, the work by van der Avoird and co-workers [22,32] emphasized the inadequacy of quasi-harmonic approaches to the crystal dynamics even in the ordered phases.

The adopted intermolecular potentials range from simple atom–atom models [19,33,34] to anisotropic models like the Kobashi and Kihara potential [27] and often include the electrostatic interactions either as point quadrupoles [21,23] or as point charges [24,25] located on the molecules.

Recent lattice dynamics calculations [25] pointed out how in nitrogen, like in most molecular crystals, the high-order electrostatic multipoles may critically affect the torsional properties of the system.

4. Anharmonic lattice dynamics calculations

While many efforts have been made for a proper account of the molecular motions in α -N₂, very little attention has been paid insofar to the energy decay mechanisms. Namely, only Kobashi's

calculations for α - [33] and γ -nitrogen [34] were an attempt to explain the observed lineshapes in terms of phonon-phonon anharmonic interactions. These were derived from an atom-atom potential model of the Lennard-Jones type, neglecting the electrostatic interactions. Such model appears rather poor, since it is not able to stabilize the α structure of nitrogen, according to subsequent molecular dynamics calculations [29].

Recently, Berns and van der Avoird [35] proposed an intermolecular potential consisting of atom-atom and charge-charge interactions based on ab initio calculations of the N_2-N_2 interactions. The same model was then utilized by Luty et al. [32] in an SCP calculation of the anharmonic phonon frequencies. More recently, Murthy et al. [25] refined a similar potential, paying special attention to the electrostatic terms. They adopted a molecular charge distribution fitting the multipole moments up to the 6th order term, yielding a good reproduction of the experimental phonon frequencies.

We have performed our anharmonic calcu-

Table 2
Intermolecular potentials for α - N_2 ^{a)}

	5q	L	E
electrostatic			
q_0 ^{b)}	-2.380	0.0	-1.3262
q_1	5.237	0.373	2.9216
q_2	-4.047	-0.373	-2.2585
r_1	± 0.549	± 0.847	± 0.672
r_2	± 0.6527	± 1.044	± 0.7994
atom-atom ^{c)}			
A	503542	144030	470000
B	-	4.037	-
C	377.6	336.3	377.6

^{a)} Quantities expressed in kcal mole⁻¹, Ångstrom and electronic units.

^{b)} Charge placed on the molecular centre of mass.

^{c)} The atom-atom interactions have the form $A/r^{12} - C/r^6$ for models 5q and E, and the form $A \exp[-Br] - C/r^6$ for model L.

lations for the last two models, here referred to as model L and model 5q respectively. The parameters characterizing these models are summarized in table 2.

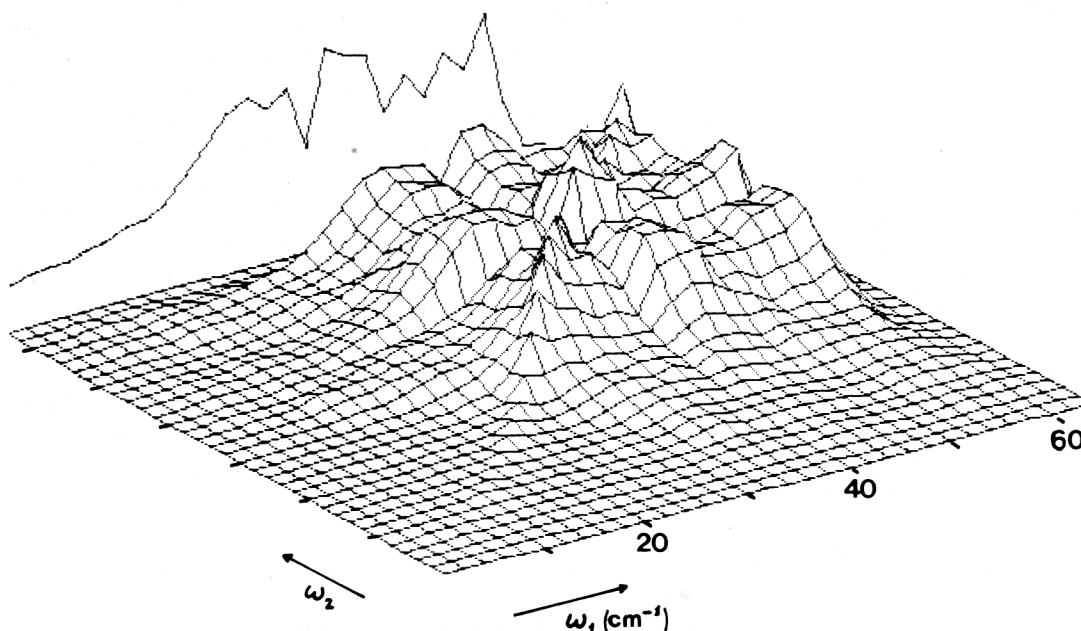


Fig. 1. One-phonon and two-phonon density of states of α - N_2 . The two-phonon density of states is defined as $\Phi_{jh}^{(2)} = \sum_{klm} \delta(\omega_{jk} - \omega_l) \delta(\omega_{mh} - \omega_k)$ and is a function of the phonon frequencies ω_l and ω_h . This and the following plots (figs. 2-4) have been smoothed and normalized, and are based on model 5q for α - N_2 (see the text for more details).

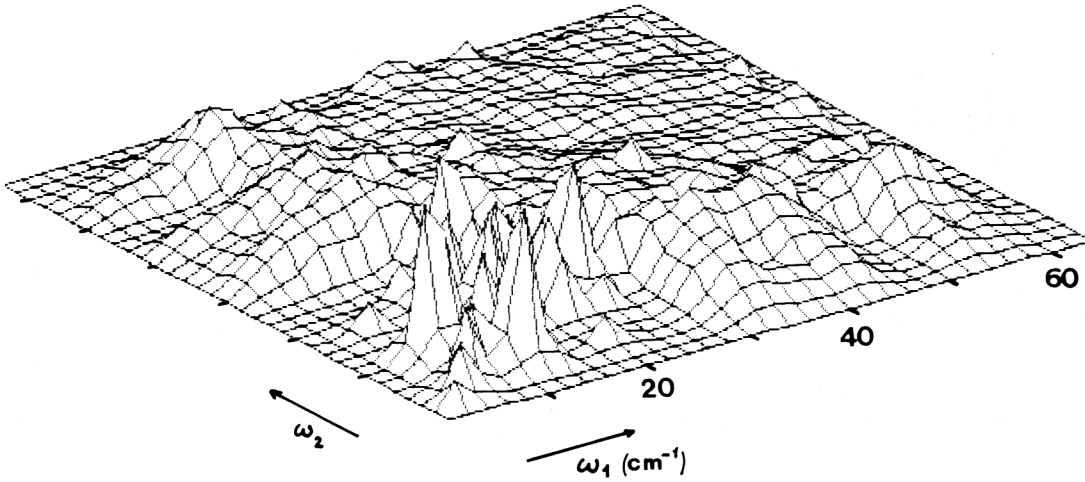


Fig. 2. Averaged third-order coupling coefficient. For each centre zone mode i , the average squared coupling coefficient is defined as $|B_{ijh}^{(3)}|^2 = [\sum_{klm} |B^{(3)}(i0, lk, m-k)|^2 \delta(\omega_{lk} - \omega_j) \delta(\omega_{m-k} - \omega_h)] / \Phi_{jh}^{(2)}$, and is a function of the phonon frequencies ω_j and ω_h . The plot shown here is an average with respect to all the centre zone modes i .

The phonon self-energy $\Sigma(\omega)$ was calculated from expressions (4a)–(4c). Its value is determined in a complex way by the number of the available states, the magnitude of the coupling coefficients, the average phonon populations and the energy conservation requirements. In the present calculations, the dampings $\Gamma^{(3)}(\omega)$ were obtained from a grid of 120 wave vectors in the reduced Brillouin

zone (1/48 of the full zone), while the frequency shifts $\Delta^{(3)}(\omega) + \Delta^{(4)}$, requiring a longer computation time, were calculated for twenty points in the reduced zone.

Although the analytic form of expressions (4a)–(4c) depends on the details of the vibrational spectrum of each crystal, similarities can be drawn for most systems. We paid special attention in

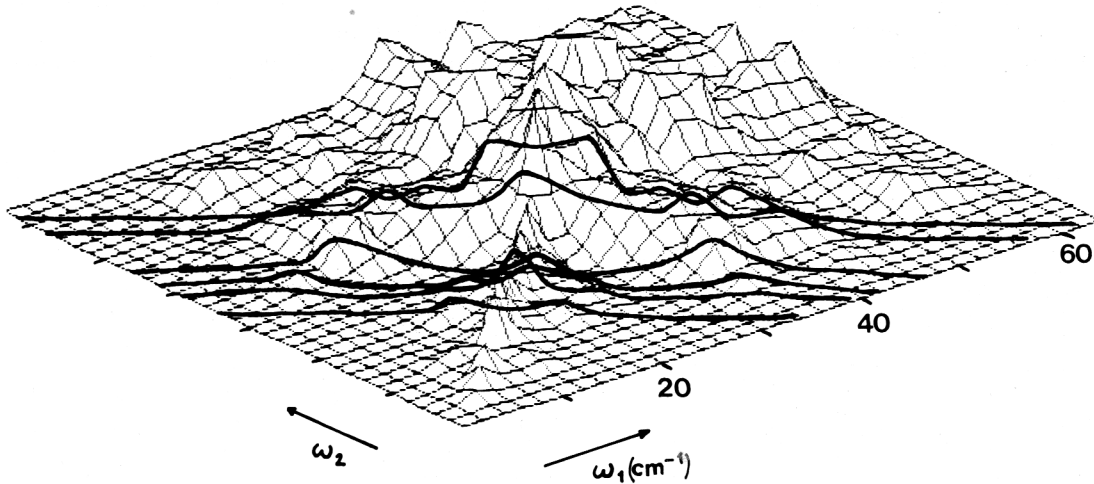


Fig. 3. Contribution to the third-order damping due to the sum processes. For each couple of frequencies ω_j and ω_h , the plot reproduces the quantity $|B_{ijh}^{(3)}|^2 \Phi_{jh}^{(2)} [n_j + n_h + 1]$ averaged over all the centre zone modes i . Only the resonant pairs with $\omega_i = \omega_j + \omega_h$ contribute to $\Gamma_i^{(3)}$ (cross sections of the plot represented by bold lines).

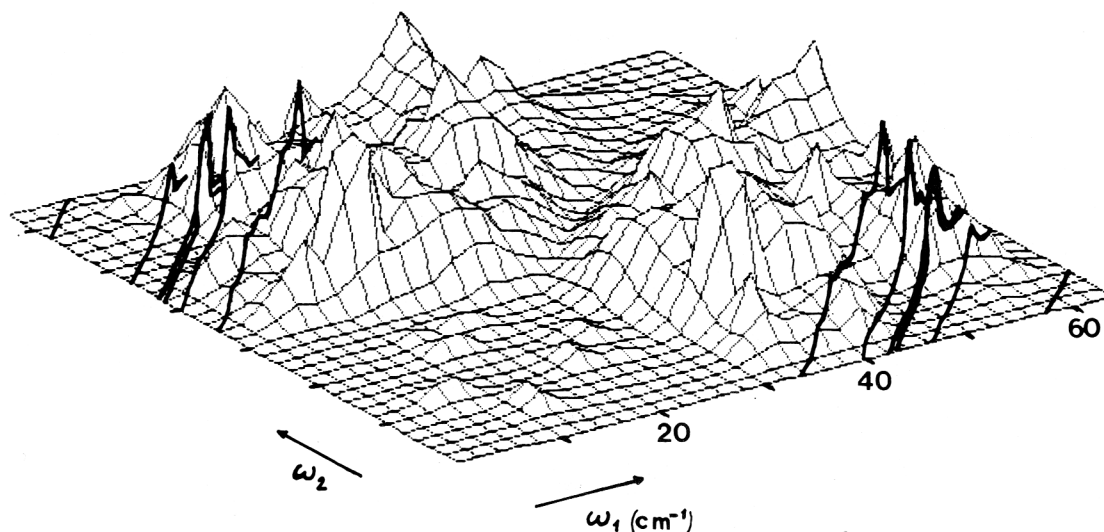


Fig. 4. Contribution to the third-order damping due to the difference processes. For each couple of frequencies ω_j and ω_h , the plot reproduces the quantity $|B_{ijh}^{(3)}|^2 \Phi_{jh}^{(2)} [n_j - n_h]$ averaged over all the centre zone modes i . Only the resonant pairs with $\omega_i = \omega_h - \omega_j$ contribute to $\Gamma_i^{(3)}$ (cross sections of the plot represented by bold lines).

analyzing the nature of the third-order decay term (4a). Figs. 1–4 are, respectively, the plots of the one- and two-phonon densities of states, of the averaged third-order coupling coefficients $|B_{ijh}^{(3)}|^2$ and of the contributions to $\Gamma^{(3)}(\omega)$ due to sum and difference processes (for more details see the figure captions).

The two-phonon density of states and the average coupling coefficient are both characterized by irregular “plateaux”, due to the contributions arising from the bulk of the Brillouin zone, with steep

slopes where the acoustic phonons with small wave vectors are involved.

At low frequencies the asymptotic behaviour of these quantities may be obtained with the long-wave method [36]. This yields expressions which depend on powers of the wave vector k . In particular, we find that the two-phonon density of states $\Phi_{ij}^{(2)}$ and the squared third-order coefficient $|B_{ijh}^{(3)}|^2$ show, respectively, a quadratic and linear dependence on the frequency ω .

At higher frequencies the effect of the fluctua-

Table 3
Harmonic and anharmonic phonon frequencies in α -N₂ ^{a)}

Mode	5q		L			E		K ^{c)}		Exp. ^{d)}
	ω	$\omega + \Delta$	ω	$\omega^{b)}$	$\omega + \Delta^{b)}$	ω	$\omega + \Delta$	ω	$\omega + \Delta$	
F _u	66.2	76.3	77.5	58.5	72.0	62.2	76.0	67.1	80.0	69
E _u	49.4	53.0	57.6	44.2	53.5	46.6	49.5	50.4	54.3	54
F _u	44.7	49.9	52.0	40.0	48.4	42.5	46.3	45.5	50.9	48
A _u	46.3	50.9	52.4	41.7	48.8	42.1	46.8	42.6	47.8	47
F _g	70.1	70.6	74.3	64.4	70.3	57.8	59.2	45.8	51.8	60
F _g	45.8	50.2	50.7	42.2	48.5	39.5	43.2	37.8	42.5	36
E _g	37.8	47.6	40.8	34.3	39.5	33.9	43.5	33.6	40.2	33

^{a)} The frequencies are expressed in cm^{-1} ; the calculated values refer to the experimental lattice constant $a = 5.644 \text{ \AA}$.

^{b)} Calculated for the minimum free energy cell, $a = 5.796 \text{ \AA}$.

^{c)} Kobashi's results, ref. [33].

^{d)} Neutron diffraction data, ref. [16].

Table 4
Measured and calculated linewidths in α -N₂ (cm⁻¹)

Mode	Exp. ^{a)}		5q	L	E	K ^{b)}
	ω	2Γ	2Γ	2Γ	2Γ	2Γ
F _u	69	6	11.1	11.6	13.4	12.6
E _u	54	—	1.9	2.5	3.1	1.9
F _u	48	0.5	1.2	1.4	1.9	1.3
A _u	47	—	1.0	1.1	1.3	0.7
F _g	60	5	7.2	7.7	7.9	5.6
F _g	36	0.8	1.2	1.3	1.5	1.3
E _g	33	0.8	0.6	0.6	0.7	1.0

^{a)} Refs. [13,15].

^{b)} Kobashi's results, ref. [33].

tions of both $\Phi_{jh}^{(2)}$ and $|B_{ijh}^{(3)}|^2$ is smoothed out by the sums over the modes and the wave vectors.

4.1. Phonon linewidths

The phonon linewidths $\Gamma_i(\omega)$ involve averages along resonant ($\omega_i = \omega_j \pm \omega_h$) cross sections of $|B_{ijh}^{(3)}|^2 \Phi_{jh}^{(2)}$ (see figs. 3 and 4) weighted by the proper (sum or difference) thermal factor.

The dominant contribution to the sum processes comes from the bulk of the two-phonon density of states, with ω_j roughly equal to ω_h .

The contributions to the difference processes arising from the central regions is effectively reduced by the thermal factors, while the low populations and the weaker coupling of the peripheral regions (involving acoustic phonons) make them unimportant.

A similar structure for the decay processes was found in crystalline naphthalene [37] and, indeed,

is expected to be typical for the lattice modes region of most molecular solids.

In tables 3–5; we report the calculated shifts and linewidths obtained from the potentials L and 5q, together with the results of Kobashi [33]. As usual in this kind of calculations (NH₃ [38], naphthalene [37], anthracene [39], α -CO [40]) the calculated linewidths follow rather closely the pattern of the thermally averaged two-phonon density of states (see fig. 5). It should be stressed, however, that these characteristics are no more satisfied when the internal modes are involved. In this case, the magnitude of the coupling coefficients, and its variations over the Brillouin zone, critically affect the results, as found in crystalline benzene [41] and naphthalene [42].

Two relevant conclusions for the dampings $\Gamma(\omega)$ can be pointed out by comparing the results of table 4:

(i) In spite of the differences between the poten-

Table 5
Calculated anharmonic shifts in α -N₂ (cm⁻¹)

Mode	5q		L		E		K ^{a)}	
	Δ^3	Δ^4	Δ^3	Δ^4	Δ^3	Δ^4	Δ^3	Δ^4
F _u	-5.1	15.2	-5.3	13.8	-6.1	16.6	-4.1	17.0
E _u	-6.6	10.2	-7.1	9.2	-7.9	11.3	-7.3	11.3
F _u	-4.5	9.7	-4.8	8.8	-5.5	10.3	-5.3	11.0
A _u	-3.8	8.4	-4.0	7.6	-4.3	9.8	-4.6	10.1
F _g	-6.3	6.8	-7.3	6.5	-6.1	8.2	-8.5	14.8
F _g	-7.2	11.6	-7.6	11.3	-8.4	13.8	-8.5	13.8
E _g	-3.8	13.6	-4.2	13.2	-4.3	16.1	-6.3	13.4

^{a)} Kobashi's results, ref. [33].

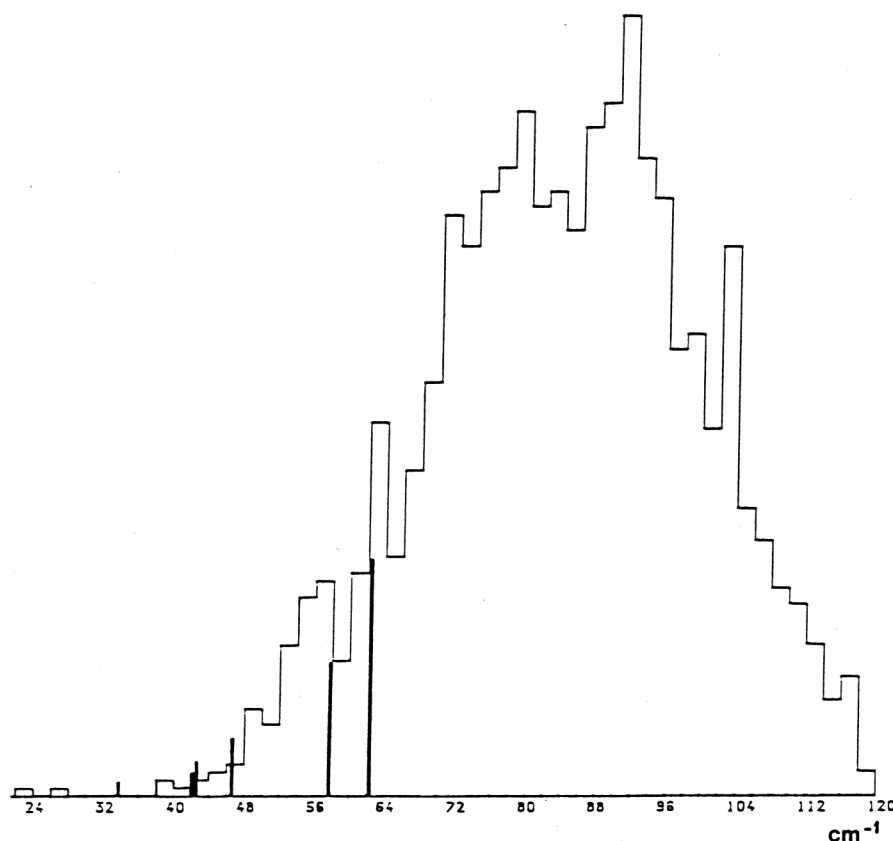


Fig. 5. Total (sum and difference) two-phonon density of states for α -N₂. The width of the phonon bands is represented by vertical lines of height proportional to the calculated linewidth.

tial models and between the calculated harmonic frequencies, the three potentials predict very similar linewidths.

(ii) The calculated linewidths compare satisfactorily to the available experimental data (table 4). The overall agreement results positively better than obtained in other systems, like ammonia [38], naphthalene [37] and anthracene [39].

4.2. Frequency shifts

An evaluation of the results for the anharmonic frequency shifts cannot be done in the same terms as for the linewidths, since no experimental observable can be directly related to $\Delta(\omega)$; the Raman spectra measured by Medina and Daniels [15], however, show that the librational frequencies

decrease slightly by increasing the temperature at constant volume. Negative anharmonic shifts are then expected at 5 K, at least for the librational modes.

The results obtained by us for the models L and 5q are collected, together with the results of Kobashi's calculations, in table 5. As already found for the dampings, the differences between the three calculations are rather small: the cubic shifts $\Delta^{(3)}$ are in all cases negative, while the quartic contributions $\Delta^{(4)}$ are all positive, and in general much larger in their absolute value. As a result, large positive shifts are predicted for almost all the optical phonons, and positive temperature shifts are calculated up to 40 K.

The results obtained for the model L apparently contradict to the calculations by Luty et al. [32],

who reported self-consistent phonon frequencies lower than the harmonic values. However, it must be stressed that the SCP frequencies were calculated at a unit cell volume larger by 6.3% than the experimental volume; if the harmonic frequencies are calculated at the reduced density, large positive shifts are obtained, similar in value to the $\Delta^{(4)}$ shifts obtained with the perturbative method (the SCP method in fact corresponds to a first-order perturbative approach, and does not include the contributions from odd anharmonic terms).

A remarkable result of our calculations is that, independent of the potential model adopted, the perturbative method gives positive anharmonic shifts for all the $\mathbf{k} = \mathbf{0}$ modes; the overall agreement of the calculated and observed frequencies is then even worse than in the harmonic approximation, particularly for the librational modes. As already mentioned, such a behaviour is a consequence of the very large quartic anharmonicity.

We attempted to improve the agreement by modifying the intermolecular potential parameters: with relatively small changes in the charge distribution and in the atom-atom parameters (potential E in table 2), we obtained lower harmonic frequencies maintaining a good fit to the unit cell volume and to the lattice energy. However, the results of the anharmonic calculations with potential E (tables 4 and 5) are not encouraging: the softening of the interaction potential causes larger librational amplitudes, resulting in larger anharmonic shifts and linewidths. It appears unlikely that remarkable improvements of the calculated anharmonic frequencies can be obtained by acting on the parameters of the intermolecular potential.

4.3. Thermal dependence of the self-energy

The self-energy (4) depends explicitly on the crystal temperature through the phonon occupations numbers. At high temperatures (i.e. $k_B T/\hbar$ larger than the lattice frequencies) the occupation numbers, and consequently the self-energy, become linear in T . At low temperatures ($k_B T/\hbar$ in the region of the acoustic frequencies) only the acoustic modes are appreciably populated. In this case, the contributions due to these long wave

modes may be evaluated by substituting the asymptotic ($\mathbf{k} \rightarrow \mathbf{0}$) expressions into (4) and replacing the sum over the wave vectors with an integral whose range, for $T \rightarrow 0$ K, may be extended to infinity [43]. The self-energy takes the form:

$$\Sigma(T) \propto T^4 + \text{constant}, \quad (6)$$

where the constant (originated from the Planck's statistics of the phonon distribution) accounts for the effect of the zero-point phonon bath. Actually, it is experimentally observed [44,45] that, for $T \rightarrow 0$ K, the phonon linewidths approach a finite value with a power law. In fig. 6 we report the temperature dependence of the linewidths for one lattice mode of α -N₂: the line a is calculated according to

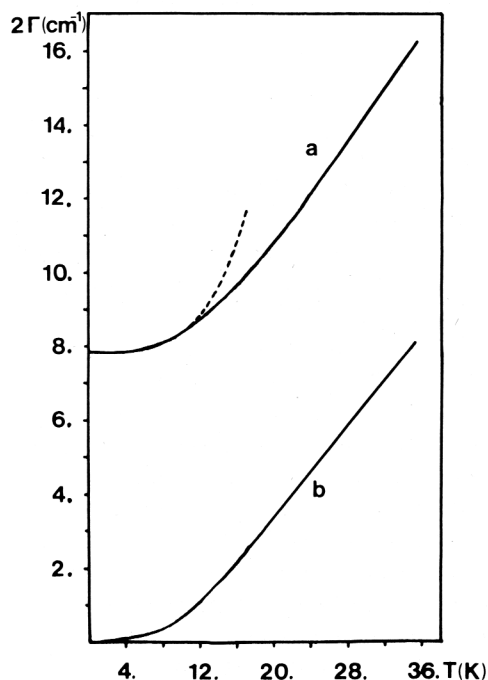


Fig. 6. Thermal dependence of the phonon linewidth for the F_g^+ mode of α -N₂. Only the effect of the temperature over the phonon populations is taken into account (no thermal expansion). The line a is derived from expression (4a), where the phonons obey the Planck's statistics; below 20 K it is evident the effect of the zero-point phonon bath, yielding the approach to a finite value with a T^4 law (the dotted line is a fit of a quartic to our calculations). The line b, on the other hand, is obtained by imposing the Boltzmann statistics to the phonon populations, thus yielding the classical prediction.

expressions (4), while the line b has been calculated by substituting the Boltzmann to the Planck statistics, thus obtaining the classical prediction where no effect of the zero-point bath is involved, and which can be compared directly to the low temperature MD results.

In analyzing the theoretical predictions, one must not forget, however, that the magnitude of the phonon self-energy, and its thermal dependence, is determined by the details of the whole phonon distribution. Moreover, when large intervals of temperature are considered, other factors (e.g., the lattice expansion) may affect the self-energy behaviour, by introducing a thermal dependence of the anharmonic couplings. This calls for caution when oversimplified models are used to account for the observed data, in order to avoid the need of meaningless hypotheses [45].

5. Discussion

The results of the anharmonic lattice dynamics calculations reported in the present paper, and those obtained by Kobashi, suggest that the anharmonic effects in α -nitrogen do not depend substantially on the adopted potential. This of course is true within the limits of the simple models utilized in the present calculations: relevant changes in the potential, like the inclusion of anisotropic atom-atom interactions (that have been shown to be important for other linear molecules), or a different analytic form of the repulsive part of the atom-atom functions, corresponding to a more realistic description of the hard-core interactions, may lead to different results. In such cases the possibility of a substantial improvement of the agreement cannot be ruled out.

The agreement with the experimental data is reasonably good as far as the linewidths (depending on the cubic anharmonicity only) are concerned; on the other hand, the experimental evidence indicates that negative anharmonic shifts should be expected, in contrast with the results of our calculations.

Other methods, different from lattice dynamics, have been previously employed in order to derive the anharmonic phonon frequencies for α -nitro-

gen. As mentioned before, van der Avoird et al. [22] utilized the same L potential of table 2 to calculate the librational and translational energy levels of the crystal with the time-dependent RPA. The method, based on the calculation of the single-libron potential well in the mean field of the other librating molecules, does not require any expansion of the intermolecular potential and does not imply any approximation as far as the potential energy is concerned. As a consequence, it avoids all the problems related to the convergence of the potential energy expansion series, that affect any lattice dynamics treatment; on the other hand, it cannot account for the decay of the vibrational energy. This method gives frequencies lower than the harmonic frequencies calculated with the same potential, in agreement with the experimental evidence.

A similar result is obtained by Cardini et al. in a molecular dynamics (MD) calculation utilizing the 5q potential [29]. Of course, MD being a classical method, the vibrational amplitudes decrease with the temperature and become vanishingly small in the vicinity of $T=0$. At 5 K, the calculated vibrational amplitudes are too small and the molecules "see" the very bottom of the potential wells; as expected, the phonon frequencies obtained from the simulation are identical to the harmonic values. However, information on the anharmonicity of the system can be obtained by rising the temperature of the computer experiment at constant volume: above 25 K the molecular displacements are large enough to sample regions of the potential well with appreciable anharmonic deformations, and small negative shifts of the phonon frequencies are obtained, in qualitative agreement with the experiment and with van der Avoird results, and in contrast with our and Kobashi's predictions.

At first, these results seem to point out the inadequacy of the perturbative approach in the α -nitrogen crystal. The values given in table 5 for $\Delta^{(3)}$ and $\Delta^{(4)}$ by themselves confirm this conclusion: 10–15 cm^{-1} shifts cannot be considered as "perturbations" to harmonic frequencies of about 50–70 cm^{-1} , and suggest that the convergence of the diagram expansion is far from being reached after the first-order quartic term. Higher-order

terms, neglected in the present calculation, might yield negative contributions to the frequency shifts, thus compensating for the very large positive effects of the terms depending on V_4 . On the other hand, the linewidths, depending in our treatment on the cubic anharmonicity only, agree satisfactorily with the experiment. A possible scenario explaining this apparent contradiction is the following:

(i) The linewidth is correctly accounted for by the cubic terms only: the potential model and the simple perturbation approach give the correct order of magnitude for the coupling between the different phonons. The importance of higher-order (four phonons and more) coupling processes, that in principle could be not negligible in view of the large values of the corresponding terms of the potential expansion, is drastically reduced by the resonance conditions (Dirac δ -functions). The relevant three-phonon density of states in the region corresponding to the $k = 0$ phonons of nitrogen, ranging between 30 and 70 cm^{-1} , is in fact relatively small and involves essentially acoustic phonons, whose coupling to the optical phonons is known to be small.

(ii) On the other hand, truncating the potential expansion at the quartic term prevents from repro-

ducing correctly the “single phonon” potential well, overestimating its anharmonic deformation and hence predicting too large shifts with respect to the harmonic frequencies.

A final issue worth considering is the role played by the translation–rotation coupling. Some insight can be drawn by comparing solid nitrogen to solid carbon monoxide, two systems traditionally considered very similar in their behaviour. We have recently proposed a model for condensed CO which was first derived from lattice dynamics calculations for the cubic phase α [40], and subsequently employed in constant pressure molecular dynamics calculations for the same phase, for the plastic phase β and the liquid phase [46]. When compared to α -CO, α -N₂ is characterized experimentally by distinctively lower frequencies and narrower lines. The disordered phase β , in which the N₂ molecules undergo a continuous motion around the c axis, exists for a rather large temperature interval (from 35.6 to 63.1 K at vapour pressure), while the analogous phase of CO exists only between 61.5 and 68.1 K. This likely denotes the effect of stronger translation–rotation couplings in this latter system, due to the asymmetry of the CO molecule, allowing to easily overcome the rotational barrier only when the system is close to

Table 6
Anharmonic lattice dynamics of α -N₂ and α -CO

Mode	ω_{harm}	Δ^3	Δ^4	$2\Gamma_{\text{anharm}}$	ω_{exp}	$2\Gamma_{\text{exp}}$
α -CO ^{a)}						
F	114.6	−5.6	6.8	22.0	90.5	7
F	84.9	−11.6	8.9	9.6	85.0	12
E	72.7	−6.0	9.6	8.6	64.5	—
F	59.2	−7.8	14.1	13.4	58.0	—
A	48.3	−4.7	5.1	2.6	—	—
F	46.4	−7.5	7.8	8.0	52(49)	5 (7)
E	43.4	−11.1	11.4	7.7	44.0	—
α -N ₂ ^{b)}						
F _u	66.2	−5.1	15.2	11.1	69.0	6
E _u	49.4	−6.6	10.2	1.9	54.0	—
F _u	44.7	−4.5	9.7	1.2	48.0	0.5
A _u	46.3	−3.8	8.4	1.0	47.0	—
F _g	70.1	−6.3	6.8	7.2	60.0	5
F _g	45.8	−7.2	11.6	1.2	36.0	0.8
E _g	37.8	−3.8	13.6	0.6	33.0	0.8

^{a)} From ref. [40].

^{b)} Present results for model 5q.

melting. Actually, α -CO is characterized by a strong mixing of the modes. The stability of the cubic phase was found to be largely affected by the magnitude of these couplings, reflected also by the anomalous acoustic dispersion [40,47], absent in α -N₂.

In table 6 our anharmonic results for both CO and N₂ are compared. In both systems the centre zone phonons decay prevalently towards $k \neq 0$ modes of mixed rotational-translational character. The stronger couplings in the less symmetric CO give origin to a higher decay rate (and, thus, to larger linewidths) when compared to the N₂ case, as found experimentally. A remarkable difference between the two calculations is in the magnitude of the quartic shifts, which in α -CO are of the same order (and opposite sign) as the third-order ones, yielding rather small corrections to the harmonic frequencies. If one considers the higher frequencies characterizing carbon monoxide, we may conclude that the dynamics of the CO molecules (while being dominated by decay processes, due to the larger translation-rotation coupling of the modes) is less affected by the stationary anharmonicity than the nitrogen case. This is a further indication that the similarity between these two systems is less extensive than usually assumed.

Acknowledgement

This work was supported by the Italian CNR and Ministero della Pubblica Istruzione. We are indebted to S. Califano, G. Cardini, M.L. Klein and S.F. O'Shea for several stimulating discussions.

References

- [1] S. Califano, V. Schettino and N. Neto, Lattice dynamics of molecular crystals (Springer, Berlin, 1981).
- [2] A.L. Fetter and J.B. Walecka, Quantum theory of many particle systems (McGraw-Hill, New York, 1971).
- [3] D.N. Zubarev, Soviet Phys. Usp. 3 (1960) 320; A.I. Alekseev, Soviet Phys. Usp. 4 (1961) 23.
- [4] A.A. Maradudin and A.E. Fein, Phys. Rev. 128 (1962) 2589.
- [5] W.M. Gelbart, in: Intermolecular spectroscopy and dynamical properties of dense systems, ed. J. van Kranendonk (North-Holland, Amsterdam, 1980).
- [6] R.A. Cowley, Advan. Phys. 12 (1963) 421; R.A. Cowley, Rept. Progr. Phys. 31 (1968) 123; T.H.K. Barron and M.L. Klein, in: Dynamical properties of solids, eds. G.K. Horton and A.A. Maradudin (North-Holland, Amsterdam, 1974).
- [7] J.O. Clayton and W.F. Giauque, J. Am. Chem. Soc. 54 (1932) 2610; W.F. Giauque and J.O. Clayton, J. Am. Chem. Soc. 55 (1933) 4875.
- [8] J.A. Venables and C.A. English, Acta Cryst. B30 (1974) 929.
- [9] A.F. Schuch and R.L. Mills, J. Chem. Phys. 52 (1970) 6000; I.N. Krupskii, A.I. Prokhvatilov and A.I. Erenburg, Fiz. Nizkikh Temp. 1 (1975) 359; D.T. Cromer, R.L. Mills, D. Schiferl and L.A. Schwable, Acta Cryst. B37 (1981) 8.
- [10] S. Buchsbaum, R.L. Mills and D. Schiferl, J. Phys. Chem. 88 (1984) 2522.
- [11] T. Scott, Phys. Rept. 27C (1976) 89.
- [12] B.P. Stoicheff, Can. J. Phys. 32 (1954) 630.
- [13] A. Anderson and G.E. Leroi, J. Chem. Phys. 45 (1966) 4359; A. Ron and O. Schnepp, J. Chem. Phys. 46 (1967) 3991; R.V. St Louis and O. Schnepp, J. Chem. Phys. 50 (1969) 5177.
- [14] A. Anderson, T.S. Sun and M.C.A. Donkersloot, Can. J. Phys. 48 (1970) 2265; B.M. Mathay and E.J. Allin, Can. J. Phys. 49 (1971) 1973.
- [15] F.D. Medina and W.B. Daniels, J. Chem. Phys. 64 (1976) 150.
- [16] J.K. Kjems and G. Dolling, Phys. Rev. B11 (1975) 1639.
- [17] J.R. Brookeman, P.C. Canepa, M.M. McEnnan and T.A. Scott, Phys. Letters 31A (1970) 404; J.R. Brookeman, M.M. McEnnan and T.A. Scott, Phys. Rev. B4 (1971) 366.
- [18] B.C. Kohin, J. Chem. Phys. 33 (1960) 882.
- [19] D.A. Goodings and M. Henkelman, Can. J. Phys. 49 (1971) 2898; P.V. Dunnmore, Can. J. Phys. 55 (1977) 554; D.A. Goodings, Can. J. Phys. 55 (1977) 73.
- [20] M.M. Thiery and V. Chandrasekharan, J. Chem. Phys. 67 (1977) 3659.
- [21] J.C. Raich, N.S. Gills and A.B. Anderson, J. Chem. Phys. 61 (1974) 1399.
- [22] A.B.J. Jansen, N.J. Briels and A. van der Avoird, J. Chem. Phys. 81 (1984) 3648; A. van der Avoird, W.J. Briels and A.P.J. Jansen, J. Chem. Phys. 81 (1984) 3658; W.J. Briels, A.P.J. Jansen and A. van der Avoird, J. Chem. Phys. 81 (1984) 4118.
- [23] T.N. Antrygina, V.A. Slusonev, Yu.A. Freiman and A.I. Erebug, J. Low Temp. Phys. 56 (1984) 331.
- [24] C.S. Murthy, K. Singer, M.L. Klein and I.R. McDonald, Mol. Phys. 41 (1980) 1387.
- [25] C.S. Murthy, S.F. O'Shea and I.R. McDonald, Mol. Phys. 50 (1983) 531.

- [26] J.C. Raich and N.J. Gillis, *J. Chem. Phys.* 66 (1977) 846.
- [27] K. Kobashi and T. Kihara, *J. Chem. Phys.* 72 (1980) 378.
- [28] M.L. Klein, D. Levesque and J.J. Weis, *Can. J. Phys.* 59 (1981) 530.
- [29] G. Cardini and S.F. O'Shea, *Phys. Rev.*, submitted for publication.
- [30] J.J. Weis and M.L. Klein, *J. Chem. Phys.* 63 (1975) 2869; M.L. Klein and J.J. Weis, *J. Chem. Phys.* 67 (1977) 217; S. Nose and M.L. Klein, *Phys. Rev. Letters* 50 (1983) 1207.
- [31] B. Kuchta, *Mol. Phys.* 52 (1984) 795.
- [32] T. Luty, A. van der Avoird and R.M. Berns, *J. Chem. Phys.* 73 (1980) 5305.
- [33] K. Kobashi, *Mol. Phys.* 36 (1978) 225.
- [34] K. Kobashi and V. Chandrasekharan, *Mol. Phys.* 36 (1978) 1645.
- [35] R.M. Berns and A. van der Avoird, *J. Chem. Phys.* 72 (1980) 6107.
- [36] R.G. Della Valle, P.F. Fracassi and S.H. Walmsley, *Chem. Phys.* 62 (1981) 231.
- [37] R.G. Della Valle, P.F. Fracassi, R. Righini and S. Califano, *Chem. Phys.* 74 (1983) 179.
- [38] R.G. Della Valle, P.F. Fracassi, R. Righini, S. Califano and S.H. Walmsley, *Chem. Phys.* 44 (1979) 189.
- [39] G. Signorini, R.G. Della Valle, P.F. Fracassi, R. Righini and S. Califano, to be published.
- [40] P.F. Fracassi, R. Righini, R.G. Della Valle and M.L. Klein, *Chem. Phys.* 96 (1985) 361.
- [41] R. Righini, P.F. Fracassi and R.G. Della Valle, *Chem. Phys. Letters* 97 (1983) 308.
- [42] R. Righini, *Chem. Phys. Letters* 84 (1983) 97.
- [43] P. Debye, *Ann. Physik* 39 (1912) 789.
- [44] J.W. Schmidt and W.B. Daniels, *J. Chem. Phys.* 73 (1980) 4848.
- [45] K. Ishi and S. Takahashi, *J. Chem. Phys.* 82 (1985) 1476.
- [46] P.F. Fracassi, M.L. Klein, R.W. Impey and G. Cardini, to be published.
- [47] P.F. Fracassi and M.L. Klein, *Chem. Phys. Letters* 108 (1984) 359.